European Journal of Mechanics B/Fluids 28 (2009) 253–258

Contents lists available at ScienceDirect

European Journal of Mechanics B/Fluids

www.elsevier.com/locate/ejmflu

Limiting behavior of micropolar flow due to a linearly stretching porous sheet

Tarek M.A. El-Mistikawy

Department of Engineering Mathematics and Physics, Faculty of Engineering, Cairo University, Giza 12211, Egypt

ARTICLE INFO

Article history:
Received 15 September 2007
Received in revised form 3 February 2008
Accepted 14 May 2008
Available online 27 May 2008

Keywords:
Micropolar flow
Stretching sheet
Suction and injection
Limiting behavior
Coordinate straining

ABSTRACT

The boundary layer flow of a micropolar fluid due to a linearly stretching sheet is studied in the limit of a vanishing coupling parameter. Asymptotic expansions of the stream function and the micro-rotation are sought after. The straightforward expansions involve secular terms. This singular behavior is removed by the novel approach of replacing the coordinate, measuring distances normal to the sheet, by two strained coordinates. This makes it possible to obtain exact (series) solutions for all levels of approximation. One can obtain results, as accurate as one would wish, by retaining enough terms of the expansions. Suction and injection through the sheet are included.

1. Introduction

The theory of micropolar fluids [3] describes the flow of a class of non-Newtonian fluids that are endowed with micro-inertia. This allows the fluid to withstand stress and body couples. The equations governing the flow of a micropolar fluid involve a micro-rotation field, in addition to the familiar velocity field. The two fields are coupled through a viscosity parameter. When this parameter vanishes, the two fields are uncoupled. The velocity field is, then, governed by the Newtonian flow equations.

When an otherwise quiescent micropolar fluid is driven by a moving flat surface, a boundary layer develops. Such flows are encountered in several practical applications; for examples, production of glass and paper sheets, drawing of plastic films, and extrusion of metals and polymers.

Self-similarity, reducing the governing partial differential equations to ordinary ones, is valid only when the surface is linearly stretching. This case was solved numerically by Hassanien and Gorla [6], who also included suction and injection. Hady [5] handled the same problem using a method of successive approximations. The Newtonian-fluid counterpart was studied by Gupta and Gupta [4].

The present work is concerned with the boundary layer flow of a micropolar fluid due to a linearly stretching flat surface. The governing equations are cast into their self-similar form; and the limiting behavior, as the coupling parameter vanishes, is explored. The leading order problem – which is the Newtonian flow case – has a closed form solution. Higher order problems, in the straightforward expansions, result in secular terms. Two sources of secularity are pinpointed; one due to the velocity field, and the other due to the micro-rotation field. In dealing with the magneto-hydrodynamic flow due to a rotating disk, El-Mistikawy et al. [1,2] encountered a secularity due to the velocity field and removed it by coordinate straining [9]. To remove the present double secularity, the similarity coordinate, measuring distances normal to the surface, is strained in two different ways. This novel treatment leads to uniformly valid expansions, the different levels of which are expressed as series solutions of the involved problems.

Numerical results based on the current asymptotic expansions are obtained for different values of the flow parameters, including cases of suction and injection. They are compared to second order accurate finite difference results. It is found that only few terms of the expansions are needed to give accurate results, even for values of the coupling parameter that are close to its upper bound.

2. Governing equations

An incompressible micropolar fluid is in steady two-dimensional motion, driven by a flat sheet that is linearly stretching away from a fixed point O. Otherwise; the fluid would have been at rest. Such a situation is encountered, for example, in glass sheet industries, when molten glass is emitted from a slot and is continuously drawn to solidify in a micropolar medium. At O, we introduce Cartesian xy-axes: the x-axis along the sheet pointing in the stretching direction, and the y-axis normal to the sheet, as shown in Fig. 1.

The velocity components (u, v) in the (x, y) directions, respectively, and the micro-rotation σ, are governed by the following boundary layer problem.

$$u_{,x} + v_{,y} = 0, \tag{1}$$

E-mail address: mistik@link.net.

0997-7546/$ – see front matter
doi:10.1016/j.euromechflu.2008.05.002

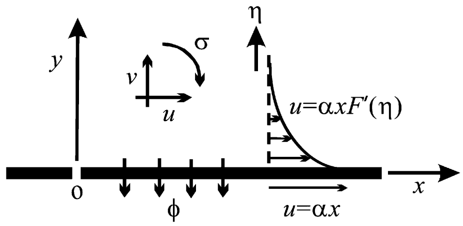

Fig. 1.

$$uu_{,x} + vu_{,y} = (\nu + \kappa)u_{,yy} + \kappa\sigma_{,y}, \tag{2}$$

$$\kappa(2\sigma + u_{,y}) = \gamma\sigma_{,yy}, \tag{3}$$

$$u = \alpha x, \quad v = -\phi, \quad \sigma = 0, \quad \text{at } y = 0, \tag{4}$$

$$u \sim 0, \quad \sigma \sim 0, \quad \text{as } y \sim \infty. \tag{5}$$

Note that a comma followed by a subscript denotes differentiation. ν, κ, and γ are kinematic viscosity coefficients associated with the rates of symmetric deformation, skew-symmetric deformation, and gyration, respectively. α is the stretching parameter. ϕ is the suction velocity through the porous surface.

The problem admits the similarity transformations

$$\eta = \alpha^{1/2}(\nu + \kappa)^{-1/2} y, \quad \psi = \alpha^{1/2}(\nu + \kappa)^{1/2} x F(\eta),$$
$$\sigma = \alpha^{3/2}(\nu + \kappa)^{-1/2} x H(\eta),$$
$$\varepsilon = \kappa(\nu + \kappa)^{-1}, \quad \beta^2 = 2\kappa(\nu + \kappa)(\alpha\gamma)^{-1},$$
$$\Phi = \alpha^{-1/2}(\nu + \kappa)^{-1/2}\phi,$$

where ψ is a stream function defined by $u = \psi_{,y}$ and $v = -\psi_{,x}$. It transforms to

$$F''' + FF'' - F'^2 = -\varepsilon H', \tag{6}$$

$$H'' - \beta^2 H = \frac{1}{2}\beta^2 F'', \tag{7}$$

$$F(0) = \Phi, \quad F'(0) = 1, \quad F'(\infty) = 0, \tag{8}$$

$$H(0) = 0, \qquad H(\infty) = 0, \tag{9}$$

where a dash denotes differentiation with respect to η, the similarity coordinate measuring distances normal to the sheet. When $\varepsilon = 0$, the velocity field is uncoupled from the micro-rotation field; so ε is a coupling parameter, that has as an upper bound the value 1.

3. Limiting behavior

We are interested in studying the limiting behavior of the flow as ε diminishes. The leading order problem corresponds to the case $\varepsilon = 0$, for which Eqs. (6) and (8), has the solution

$$F_0 = \lambda_0 - \lambda_0^{-1} e^{-\lambda_0 \eta}, \qquad \lambda_0 = \frac{1}{2}\left(\Phi + \sqrt{\Phi^2 + 4}\right) = F_0(\infty). \tag{10}$$

The corresponding solution for Eqs. (7) and (9), when $\beta \neq \lambda_0$, is

$$H_0 = \chi\left[e^{-\beta\eta} - e^{-\lambda_0\eta}\right], \qquad \chi = \frac{\frac{1}{2}\lambda_0\beta^2}{\lambda_0^2 - \beta^2}. \tag{11}$$

These represent the leading order terms in the asymptotic expansions for F and H as $\varepsilon \sim 0$. The fact that the right-hand side of Eq. (6) is $O(\varepsilon)$ suggests that the expansions proceed as follows

$$F \sim \sum_{i=0} \varepsilon^i F_i, \qquad H \sim \sum_{i=0} \varepsilon^i H_i, \tag{12}$$

where, as a convention, a summation without upper limit may extend to infinity. Substituting in Eqs. (6)–(9) and equating like powers of ε, on both sides of each equation, lead to a hierarchy of problems governing the different levels of the expansions.

For $i \geqslant 1$, the problem for F_i takes the form

$$F_i''' + \lambda_0(1 - \theta)F_i'' - 2\lambda_0^2\theta F_i' - \lambda_0^3\theta F_i = R_i, \qquad \theta = \lambda_0^{-2} e^{-\lambda_0\eta}, \tag{13}$$

$$F_i(0) = 0, \quad F_i'(0) = 0, \quad F_i'(\infty) = 0 \tag{14}$$

while that for H_i takes the form

$$H_i'' - \beta^2 H_i = \frac{1}{2}\beta^2 F_i'', \tag{15}$$

$$H_i(0) = 0, \qquad H_i(\infty) = 0. \tag{16}$$

Eq. (13) admits two successive reductions of order. Specifically, the substitution

$$F_i = e^{-\lambda_0\eta}\left(\int \bar{F}_i \, d\eta + \bar{c}_i\right) \tag{17}$$

followed by the substitution

$$\bar{F}_i = e^{\lambda_0\eta}(1 + \theta)\left(\int \hat{F}_i \, d\eta + \hat{c}_i\right) \tag{18}$$

leads to a linear first order differential equation for $\hat{F}_i$, whose solution is

$$\hat{F}_i = \frac{\int (1 + \theta)e^{\theta} R_i \, d\eta + \tilde{c}_i}{(1 + \theta)^2 e^{\theta}}. \tag{19}$$

The integration constants $\bar{c}_i$, $\hat{c}_i$ and $\tilde{c}_i$ should be determined so that F_i satisfies conditions (14). The use of Eqs. (17)–(19) is, obviously, prohibitive; specially with R_i being determined recursively. The alternative is to find expansions for F_i.

For $i = 1$, substituting

$$R_1 = \chi\left(\beta e^{-\beta\eta} - \lambda_0 e^{-\lambda_0\eta}\right), \tag{20}$$

expanding in powers of $e^{-\lambda_0\eta}$, and carrying out the integrals in Eqs. (19), (18) then (17), give an expression for F_1 that takes the form

$$F_1 \sim a_1 + b_{101} e^{-\lambda_0\eta} + \sum_{k=0} b_{11k} e^{-k\lambda_0\eta} e^{-\beta\eta} + \hat{b}_{101}\eta e^{-\lambda_0\eta}. \tag{21}$$

Note that the summation in expansion (21) converges, since it can be shown that the point at infinity η is a regular singular point of Eq. (13).

The term involving $\eta e^{-\lambda_0\eta}$ is a secular term. It causes F_1 to outgrow F_0 as $\eta \sim \infty$. Moreover, when expansion (21) for F_1 is substituted in the problem for H_1 the term involving $e^{-\beta\eta}$ causes H_1 to develop a secular term involving $\eta e^{-\beta\eta}$. These secularities are magnified in higher order problems. The problem for F_i introduces a term involving $\eta^i e^{-\lambda_0\eta}$, and that for H_i introduces a term involving $\eta^i e^{-\beta\eta}$.

To remove this double secular behavior, we employ the novel approach of straining the coordinate η in two different ways. We introduce the coordinates

$$\zeta = \lambda\eta, \qquad \xi = \mu\eta, \tag{22}$$

to handle the secularities associated with Eq. (6) for F, and Eq. (7) for H, respectively. The straining parameters λ and μ have the expansions

$$\lambda \sim \sum_{i=0} \varepsilon^i \lambda_i, \tag{23}$$

$$\mu \sim \sum_{i=0} \varepsilon^i \mu_i, \quad \mu_0 = \beta, \tag{24}$$

where the λ_i's and μ_i's (for $i = 1, 2, \ldots$) are chosen so that the secular terms vanish.

Table 1
Effect of the cutoff values I and K ($\varepsilon = 0.1$, $\beta = 0.2$, $\Phi = 0$)

I	$F''(0)$	$F(\infty)$	$F''(0)$	$F(\infty)$
	$K = 5$		$K = 10$	
1	−0.9995424078	0.9930469106	−0.9995421776	0.9930469312
2	−0.9995434052	0.9930130498	−0.9995431566	0.9930130721
3	−0.9995434221	0.9930126425	−0.9995431726	0.9930126648
4	−0.9995434224	0.9930126360	−0.9995431728	0.9930126583
5	−0.9995434225	0.9930126358	−0.9995431729	0.9930126581

The uniformly valid expansions for F and H can, now, be written as follows

$$F \sim \sum_{i=0} \varepsilon^i \left(a_i + b_{i01} e^{-\zeta} + b_{i10} e^{-\xi}\right) + \sum_{i=1} \varepsilon^i \sum_{j=1}^{i} \sum_{k=1} b_{ijk} e^{-j\xi} e^{-k\zeta}, \tag{25}$$

$$H \sim \sum_{i=0} \varepsilon^i \left(c_i e^{-\zeta} + d_{i10} e^{-\xi}\right) + \sum_{i=1} \varepsilon^i \sum_{j=1}^{i} \sum_{k=1} d_{ijk} e^{-j\xi} e^{-k\zeta}. \tag{26}$$

We substitute these expressions in Eqs. (6)–(9), then equate the coefficients of $\varepsilon^i e^{-j\xi} e^{-k\zeta}$ for all possible combinations of i, j, and k. This leads to relations that can be used to determine the λ_i's, μ_i's, a_i's, b_{ijk}'s, c_i's, and d_{ijk}'s, recursively.

For $i = 0$, we get,

$$a_0 = \lambda_0, \quad b_{001} = -\lambda_0^{-1}, \quad b_{010} = 0, \quad c_0 = -\chi, \quad d_{010} = \chi$$

so that we recover expressions (10) and (11) for F_0 and H_0. For $i \geqslant 1$, the recurrence relations are given in Appendix A.

4. Sample results and assessment

Of the three parameters ε, β, and Φ, involved in Eqs. (6)–(9), the coefficients appearing in the expansions for the stream function F, the micro-rotation H, and the straining parameters λ and μ depend on β and Φ, only. For prescribed β and Φ, these coefficients can be determined using the recurrence relations given in Appendix A. They can, then, be combined with any small value of ε to give a full description of the flow field.

Two quantities of particular importance are $F''(0)$ representing the shear stress at the surface, and $F(\infty)$ representing the inflow toward the boundary layer that is needed to compensate for the flow driven by the stretching sheet. These two quantities will be the focus of the numerical values presented below.

Table 3
Effect of β ($\varepsilon = 0.1$, $\Phi = 0$)

β	$F''(0)$	$F(\infty)$	$F''(0)$	$F(\infty)$
	Asymptotic		Numerical	
0.2	−0.9995434221	0.9930126425	−0.9995431796	0.9930126330
0.4	−0.9986102203	0.9893556424	−0.9986095633	0.9893555991
0.6	−0.9975333891	0.9871332468	−0.9975318636	0.9871332066
0.8	−0.9964537113	0.9856265677	−0.9964428365	0.9856272306
1.0	–	–	−0.9953967274	0.9845232857
2.0	−0.9911562316	0.9814894147	−0.9911561519	0.9814871241
4.0	−0.9862331980	0.9790468647	−0.9862335527	0.9790465681
6.0	−0.9835601943	0.9779198339	−0.9835607175	0.9779195460
8.0	−0.9818909866	0.9772599580	−0.9818916031	0.9772596766
10.0	−0.9807503239	0.9768248764	−0.9807510021	0.9768245995

Cutoff values I and K for the counters i and k, respectively, have to be specified in such a way that does not affect the accuracy. Table 1 presents $F''(0)$ and $F(\infty)$ in the typical case ($\varepsilon = 0.1$, $\beta = 0.2$, $\Phi = 0$) at several values of I and K. It is concluded that the values $I = 3$ and $K = 5$ are quite satisfactory. They are used for all following calculations.

The coefficients for the case ($\beta = 0.2$, $\Phi = 0$) are given in Table 2. It is noted that they are well-behaved; decreasing in absolute value as the counters i and k increase. This indicates convergence of the summations on both counters.

The obtained asymptotic expansions break down when β approaches its critical value $\beta_c = \lambda_0$. Well-behaved coefficients are obtained only when β is away from β_c. Table 3 gives $F''(0)$ and $F(\infty)$, for several values of β, when $\Phi = 0$ (for which $\lambda_0 = 1$) and $\varepsilon = 0.1$. The underscored values of β behave well with k, but show growth in the coefficients as the asymptotic index i increases. This only means that we may need to use small values of ε, for few terms of the asymptotic expansions to give accurate results.

The asymptotic expansions favor suction cases ($\Phi > 0$) to injection cases ($\Phi < 0$). As Φ increases λ_0 increases, extending the subcritical range of well-behaved $\beta < \beta_c$. In Table 4, some cases of suction and injection are presented, when $\varepsilon = 0.1$ and $\beta = 0.2$.

Included, in Tables 3 and 4, are second order accurate finite difference results that are obtained using Keller's two-point method [7], with the far field conditions enforced at a finite value $\eta = \eta_\infty$. The value $\eta_\infty = 100$ and a uniform step size $\Delta\eta = 0.01$ are used throughout. The solution is obtained iteratively, and con-

Table 2
Coefficients of the typical case ($\beta = 0.2$, $\Phi = 0$)

(a)

i	λ_i	μ_i	a_i	b_{i01}	c_i	b_{i10}	d_{i10}
0	1.0	0.2	1.0	−1.0	−0.20833E−1	0.0	0.20833E−1
1	−0.90364E−1	0.12500E−1	0.69531E−1	−0.22680	0.45681E−2	−0.13021	0.13465E−2
2	−0.54255E−2	0.16724E−2	0.33861E−2	0.47817E−1	−0.99248E−3	−0.13629E−1	0.23440E−3
3	−0.73659E−3	0.29057E−3	0.40739E−3	−0.31873E−2	0.59262E−4	−0.25797E−2	0.50700E−4

(b)

k	b_{11k}	d_{11k}	b_{21k}	d_{21k}	b_{22k}	d_{22k}
1	0.289352	−0.595238E−2	−0.849436E−1	0.172534E−2	0.480562E−1	−0.981146E−3
2	−0.199278E−2	0.401878E−4	0.334429E−3	−0.669310E−5	−0.108220E−2	0.217954E−4
3	0.127379E−3	−0.255758E−5	−0.356264E−4	0.713702E−6	0.102617E−3	−0.205947E−5
4	−0.109219E−4	0.218933E−6	0.444981E−5	−0.891157E−7	−0.115651E−4	0.231780E−6
5	0.984782E−6	−0.197248E−7	−0.531530E−6	0.106414E−7	0.129064E−5	−0.258482E−7

(c)

k	b_{31k}	d_{31k}	b_{32k}	d_{32k}	b_{33k}	d_{33k}
1	0.152305E−1	−0.310129E−3	−0.155280E−1	0.315122E−3	0.586623E−2	−0.119187E−3
2	−0.158929E−3	0.320520E−5	0.235965E−3	−0.473251E−5	−0.309732E−3	0.623151E−5
3	0.178831E−4	−0.358900E−6	−0.342561E−4	0.686465E−6	0.427928E−4	−0.858505E−6
4	−0.237423E−5	0.475740E−7	0.539421E−5	−0.108034E−6	−0.629428E−5	0.126124E−6
5	0.307636E−6	−0.616009E−8	−0.777519E−6	0.155661E−7	0.865700E−6	−0.173361E−7

Table 4
Effect of Φ ($\varepsilon = 0.1$, $\beta = 0.2$)

Φ	$F''(0)$	$F(\infty)$	$F''(0)$	$F(\infty)$
	Asymptotic		Numerical	
1.0	−1.617807376	1.614837567	−1.617807388	1.614837556
0.5	−1.280439102	1.276027816	−1.280439101	1.276027799
0.0	−0.999543422	0.993012643	−0.999543180	0.993012633
−0.5	−0.780244723	0.770939861	−0.780239589	0.770940331
−1.0	−0.617577764	0.605124728	−0.617488704	0.605136212

Table 5
Effect of ε

a: ($\beta = 0.2$, $\Phi = 0$)				
ε	$F''(0)$	$F(\infty)$	$F''(0)$	$F(\infty)$
	Asymptotic		Numerical	
0.1	−0.9995434221	0.9930126425	−0.9995431796	0.9930126330
0.3	−0.9986366565	0.9788249852	−0.9986358164	0.9788244322
0.5	−0.9977390874	0.9643371093	−0.9977375636	0.9643326822
0.7	−0.9968515261	0.9495294600	−0.9968494255	0.9495117102
0.9	−0.9959747840	0.9343824825	−0.9959725656	0.9343317733
b: ($\beta = 0.8$, $\Phi = 0$)				
ε	$F''(0)$	$F(\infty)$	$F''(0)$	$F(\infty)$
	Asymptotic		Numerical	
0.1	−0.9964537113	0.9856265677	−0.9964428365	0.9856272306
0.3	−0.9895583704	0.9559439842	−0.9893284405	0.9559522823
0.5	−0.9832370860	0.9248541576	−0.9822252893	0.9248509827
0.7	−0.9778631473	0.8921655461	−0.9751520320	0.8920244869
0.9	−0.9738098436	0.8576866083	−0.9681362630	0.8570403811

Table 6
Effect of η_∞ on numerical results ($\varepsilon = 0.1$, $\beta = 0.2$, $\Phi = 0.0$)

η_∞	$F''(0)$	$F(\infty)$
10	−0.9995383038	0.9960657285
20	−0.9995403630	0.9936768025
40	−0.9995431267	0.9930303013
80	−0.9995431796	0.9930126421
100	−0.9995431796	0.9930126330
∞[a]	−0.9995434221	0.9930126425

[a] Asymptotic values.

vergence is considered reached when the absolute value of the error in $F''(0)$, in two successive iterations, does not exceed 10^{-10}. Agreement of the numerical and the asymptotic solutions is noticeable.

The asymptotic expansions proved accurate throughout the domain $(0,1)$ of the coupling parameter ε. This is demonstrated in Table 5a, which compares the asymptotic and the numerical results for different values of ε in the case ($\beta = 0.2$, $\Phi = 0$). Table 5b presents corresponding results in the case ($\beta = 0.8$, $\Phi = 0$), in which β is close to its critical value $\beta_c = 1$. Reasonable accuracy is still observed.

The obtained asymptotic expansions are useful in numerous ways. They can be used to calculate the flow variables at specific points. They can be manipulated to give quantities of practical importance, with controlled accuracy. Their accurate results can be used to judge other numerical and approximate solution methods. To make use of this last point, the effect of the value of η_∞, at which to enforce the far field conditions, has been investigated. (Use of a small value of η_∞ is a common error in boundary layer calculations, as noted by Pantokratoras [8].) Different values of η_∞ have been used, as recorded in Table 6. Considerable improvement in the numerical results is observed as η_∞ is increased. The value $\eta_\infty = 100$ mentioned earlier has been found satisfactory.

Appendix A

In this appendix, we give the relations that can be used, sequentially, to determine the λ_i's, μ_i's, a_i's, b_{ijk}'s, c_i's, and d_{ijk}'s, which appear in expansions (23)–(26), when $i > 0$. For conciseness, we define

$$\nu_{jk} = j\mu + k\lambda \sim \sum_{i=0} \varepsilon^i \nu_{ijk}, \qquad \nu_{ijk} = j\mu_i + k\lambda_i$$

and, with ω standing for λ, μ, or ν, we write

$$\omega^2 \sim \sum_{i=0} \varepsilon^i \omega_i^2, \qquad \omega_i^2 = \sum_{s=0}^{i} \omega_{i-s}\omega_s,$$

$$\omega^3 \sim \sum_{i=0} \varepsilon^i \omega_i^3, \qquad \omega_i^3 = \sum_{s=0}^{i}\sum_{r=0}^{s} \omega_{i-s}\omega_{s-r}\omega_r.$$

The following relations are to be used to determine the underlined coefficients.
For $i = 1$, we have

$$(\mu_0^3 - \lambda_0\mu_0^2)\underline{b_{110}} = -\mu_0 d_{010},$$

$$(\nu_{01k}^3 - \lambda_0\nu_{01k}^2)\underline{b_{11k}} = -\lambda_0^{-1}(\nu_{01k-1}^2 + \lambda_0^2 - 2\nu_{01k-1}\lambda_0)b_{11k-1}, \quad k \geqslant 1,$$

$$(\nu_{01k}^2 - \beta^2)\underline{d_{11k}} = \nu_{01k}^2 b_{11k}, \quad k \geqslant 1,$$

$$(1+\lambda_0^2)\underline{b_{101}} = c_0 - \sum_{k=0}(1+\lambda_0\nu_{01k})b_{11k},$$

$$\underline{a_1} = -b_{101} - \sum_{k=0} b_{11k},$$

$$\underline{\lambda_1} = c_0 + a_1,$$

$$(\lambda_0^2 - \beta^2)\underline{c_1} = -\frac{1}{2}\beta^2(\lambda_0^{-1}\lambda_1^2 - \lambda_0^2 b_{101}) - \lambda_1^2 c_0,$$

$$\underline{d_{110}} = -c_1 - \sum_{k=1} d_{11k},$$

$$2\mu_0 d_{010}\underline{\mu_1} = \frac{1}{2}\beta^2\mu_0^2 b_{110}.$$

For $i \geqslant 2$, with $n \wedge q = \max(n,q)$ and $n \vee q = \min(n,q)$, we have

$$(\mu_0^3 - \lambda_0\mu_0^2)\underline{b_{i10}} = -\mu_{i-1}d_{010} - \sum_{m=1}^{i-1}\Bigg[\mu_{i-1-m}d_{m10} + (\mu_{i-m}^3 - \lambda_0\mu_{i-m}^2)b_{m10} - \sum_{s=1}^{m}\mu_{m-s}^2 b_{s10}a_{i-m}\Bigg],$$

$$(\nu_{011}^3 - \lambda_0\nu_{011}^2)\underline{b_{i11}} = -\lambda_0^{-1}(\mu_0^2 + \lambda_0^2 - 2\mu_0\lambda_0)b_{i10} - \sum_{m=1}^{i-1}\Bigg[(\nu_{i-m11}^3 - \lambda_0\nu_{i-m11}^2)b_{m11} + \lambda_0^{-1}(\mu_{i-m}^2 + \lambda_{i-m}^2 - 2\mu_{i-m}\lambda_0)b_{m10} + \nu_{i-1-m11}d_{m11} + \sum_{s=1}^{m}\Bigg\{2\sum_{r=1}^{i-m}\mu_{m-s}\lambda_{i-m-r}b_{s10}b_{r01} - \lambda_{m-s}^2 b_{s01}b_{i-m10} - \mu_{m-s}^2 b_{s10}b_{i-m01} - \nu_{m-s11}^2 a_{i-m}b_{s11} - 2\lambda_0^{-1}\lambda_{i-m}\mu_{m-s}b_{s10}\Bigg\}\Bigg]$$

$$
\begin{aligned}
&(\nu_{01k}^3-\lambda_0\nu_{01k}^2)\underline{b_{i1k}}\\
&\quad=-\lambda_0^{-1}(\nu_{01k-1}^2+\lambda_0^2-2\nu_{01k-1}\lambda_0)b_{i1k-1}\\
&\qquad-\sum_{m=1}^{i-1}\Big[(\nu_{i-m1k}^3-\lambda_0\nu_{i-m1k}^2)b_{m1k}\\
&\qquad+\lambda_0^{-1}(\nu_{i-m1k-1}^2+\lambda_{i-m}^2-2\nu_{i-m1k-1}\lambda_0)b_{m1k-1}\\
&\qquad+\nu_{i-1-m1k}d_{m1k}+\sum_{s=1}^{m}\Big\{2\sum_{r=1}^{i-m}\nu_{m-s1k-1}\lambda_{i-m-r}b_{s1k-1}b_{r01}\\
&\qquad-\nu_{m-s1k-1}^2b_{s1k-1}b_{i-m01}-\nu_{m-s1k}^2a_{i-m}b_{s1k}\\
&\qquad-2\lambda_0^{-1}\lambda_{i-m}\nu_{m-s1k-1}b_{s1k-1}-\sum_{s=1}^{i-m}\lambda_{i-m-s}^2b_{s01}b_{m1k-1}\Big\}\Big],\\
&\quad k\geqslant 2,
\end{aligned}
$$

$$
\begin{aligned}
&(\nu_{0j1}^3-\lambda_0\nu_{0j1}^2)\underline{b_{ij1}}\\
&\quad=(\mu_0^2+\nu_{0j-11}^2-2\mu_0\nu_{0j-11})b_{j-1j-11}b_{i-j+110}\\
&\qquad-\sum_{m=j}^{i-1}\Big[(\nu_{i-mj1}^3-\lambda_0\nu_{i-mj1}^2)b_{mj1}\\
&\qquad-(\mu_{i-m}^2+\nu_{i-mj-11}^2-2\mu_{i-m}\nu_{j-110})b_{m-j+110}b_{j-1j-11}\\
&\qquad+\nu_{i-1-mj1}d_{mj1}+\sum_{s=j}^{m}\Big\{2\sum_{r=1}^{i-m}\nu_{m-sj-11}\mu_{i-m-r}b_{r10}b_{sj-11}\\
&\qquad-\nu_{m-sj-11}^2b_{sj-11}b_{i-m10}-\nu_{m-sj1}^2a_{i-m}b_{sj1}\Big\}\\
&\qquad+\sum_{s=1}^{i-m}(2\mu_{i-m-s}\nu_{m-j+1j-11}b_{j-1j-11}-\mu_{i-m-s}^2b_{mj-11})b_{s10}\Big],\\
&\quad 2\leqslant j\leqslant i-1,
\end{aligned}
$$

$$
\begin{aligned}
&(\nu_{0jk}^3-\lambda_0\nu_{0jk}^2)\underline{b_{ijk}}\\
&\quad=(\nu_{0j-1k}^2+\mu_0^2-2\nu_{0j-1k}\mu_0)b_{j-1j-1k}b_{i-j+110}\\
&\qquad-\lambda_0^{-1}(\nu_{0jk-1}^2+\lambda_0^2-2\nu_{0jk-1}\lambda_0)b_{ijk-1}\\
&\qquad-\sum_{m=j}^{i-1}\Big[(\nu_{i-mjk}^3-\lambda_0\nu_{i-mjk}^2)b_{mjk}\\
&\qquad+\lambda_0^{-1}(\nu_{i-mjk-1}^2+\lambda_{i-m}^2-2\nu_{i-mjk-1}\lambda_0)b_{mjk-1}+\nu_{i-1-mjk}d_{mjk}\\
&\qquad-(\nu_{i-mj-1k}^2+\mu_{i-m}^2-2\nu_{0j-1k}\mu_{i-m})b_{m-j+110}b_{j-1j-1k}\\
&\qquad-\sum_{s=1}^{i-m}\lambda_{i-m-s}^2b_{s01}b_{mjk-1}\\
&\qquad-\sum_{s=j}^{m}\Big\{\nu_{m-sjk}^2a_{i-m}b_{sjk}+\nu_{m-sjk-1}^2b_{i-m01}b_{sjk-1}\\
&\qquad+\nu_{m-sj-1k}^2b_{i-m10}b_{sj-1k}+2\lambda_0^{-1}\lambda_{i-m}\nu_{m-sjk-1}b_{sjk-1}\\
&\qquad-2\sum_{r=1}^{i-m}(\lambda_{i-m-r}\nu_{m-sjk-1}b_{r01}b_{sjk-1}\\
&\qquad+\mu_{i-m-r}\nu_{m-sj-1k}b_{r10}b_{sj-1k})\Big\}\\
&\qquad-\sum_{s=1}^{i-m}(\mu_{i-m-s}^2b_{mj-1k}+2\mu_{i-m-s}\nu_{m-j+1j-1k}b_{j-1j-1k})b_{s10}\Big]\\
&\qquad+\sum_{m=1}^{i-1}\sum_{p=1\wedge j-m}^{i-m\vee j-1}\sum_{s=p}^{i-m}\sum_{t=1}^{k-1}\Big(\nu_{i-m-spt}^2b_{mj-pk-t}-\nu_{i-m-spt}\\
&\qquad\times\sum_{r=j-p}^{m}\nu_{m-rj-pk-t}b_{rj-pk-t}\Big)b_{spt},\quad 2\leqslant j\leqslant i-1,k\geqslant 2,
\end{aligned}
$$

$$
(\nu_{0i1}^3-\lambda_0\nu_{0i1}^2)\underline{b_{ii1}}=(\nu_{0i-11}^2+\mu_0^2-2\nu_{0i-11}\mu_0)b_{110}b_{i-1i-11},
$$

$$
\begin{aligned}
&(\nu_{0ik}^3-\lambda_0\nu_{0ik}^2)\underline{b_{iik}}\\
&\quad=(\nu_{0i-1k}^2+\mu_0^2-2\nu_{0i-1k}\mu_0)b_{110}b_{i-1i-1k}\\
&\qquad-(\nu_{0ik-1}^2\lambda_0^{-1}+\lambda_0-2\nu_{0ik-1})b_{iik-1}\\
&\qquad+\sum_{m=1}^{i-1}\sum_{p=1\wedge j-m}^{i-m\vee j-1}\sum_{s=p}^{i-m}\sum_{t=1}^{k-1}\Big(\nu_{i-m-spt}^2b_{mj-pk-t}-\nu_{i-m-spt}\\
&\qquad\times\sum_{r=j-p}^{m}\nu_{m-rj-pk-t}b_{rj-pk-t}\Big)b_{spt},\quad k\geqslant 2,
\end{aligned}
$$

$$
\begin{aligned}
&(\nu_{0jk}^2-\beta^2)\underline{d_{ijk}}=\frac{1}{2}\beta^2\sum_{m=j}^{i}\nu_{i-mjk}^2b_{mjk}-\sum_{m=j}^{i-1}\nu_{i-mjk}^2d_{mjk},\\
&\quad 1\leqslant j\leqslant i,k\geqslant 1,
\end{aligned}
$$

$$
(\nu_{0ik}^2-\beta^2)\underline{d_{iik}}=\frac{1}{2}\beta^2\nu_{0ik}^2b_{iik},\quad k\geqslant 1,
$$

$$
\underline{\tau_1}=-b_{i10}-\sum_{j=1}^{i}\sum_{k=1}b_{ijk},
$$

$$
\begin{aligned}
\underline{\tau_2}=&\Bigg[\sum_{m=1}^{i-1}\Bigg\{\lambda_0^{-1}\Bigg(\lambda_{i-m}^2a_m-\sum_{s=0}^{m}\lambda_{i-m}\lambda_{m-s}\lambda_s\Bigg)-\sum_{s=1}^{m}\lambda_{m-s}^2b_{s01}a_{i-m}\Bigg\}\\
&+\sum_{m=0}^{i-1}\lambda_{i-1-m}c_m\Bigg]\Big/\lambda_0,
\end{aligned}
$$

$$
\begin{aligned}
(1+\lambda_0^2)\underline{b_{i01}}=\tau_1+\tau_2-\Bigg[&\mu_0b_{i10}+\sum_{m=1}^{i-1}(\lambda_{i-m}b_{m01}+\mu_{i-m}b_{m10})\\
&+\sum_{j=1}^{i}\sum_{m=j}^{i}\sum_{k=1}\nu_{i-mjk}b_{mjk}\Bigg]\lambda_0,
\end{aligned}
$$

$$
\underline{a_i}=\tau_1-b_{i01},
$$

$$
\underline{\lambda_i}=\tau_2+a_i,
$$

$$
(\lambda_0^2-\beta^2)\underline{c_i}=\frac{1}{2}\beta^2\Bigg(\sum_{m=1}^{i}\lambda_{i-m}^2b_{m01}-\lambda_0^{-1}\lambda_i^2\Bigg)-\sum_{m=0}^{i-1}\lambda_{i-m}^2c_m,
$$

$$
\underline{d_{i10}}=-c_i-\sum_{j=1}^{i}\sum_{k=1}d_{ijk},
$$

$$
2\mu_0d_{010}\underline{\mu_i}=\frac{1}{2}\beta^2\sum_{m=1}^{i}\mu_{i-m}^2b_{m10}-\sum_{m=1}^{i-1}(\mu_{i-m}^2d_{m10}+\mu_{i-m}\mu_md_{010}).
$$

References

[1] T.M.A. El-Mistikawy, H.A. Attia, A.A. Megahed, Asymptotic solution for the flow due to an infinite rotating disk in the case of small magnetic field, Mech. Res. Commun. 25 (1998) 271–278.

[2] T.M.A. El-Mistikawy, H.A. Attia, A.A. Megahed, Asymptotic solution for the flow due to an infinite rotating disk in the case of large magnetic field, Trans. CSME 24 (2000) 515–523.

[3] A.C. Eringen, Theory of micropolar fluids, J. Math. Mech. 16 (1966) 1–18.

[4] P.S. Gupta, A.S. Gupta, Heat and mass transfer on a stretching sheet with suction or blowing, Can. J. Chem. Engrg. 55 (1977) 744–746.

[5] F.M. Hady, On the solution of heat transfer to micropolar fluid from a non-isothermal stretching sheet with injection, Int. J. Numer. Meth. Heat Fluid Flow 6 (1996) 99–104.

[6] I.A. Hassanien, R.S.R. Gorla, Heat transfer to a micropolar fluid from a non-isothermal stretching sheet with suction and blowing, Acta Mech. 84 (1990) 191–203.
[7] H.B. Keller, Accurate difference methods for linear ordinary differential systems subject to linear constraints, SIAM J. Numer. Anal. 6 (1969) 8–30.
[8] A. Pantokratoras, A common error made in investigation of boundary layer flows, Appl. Math. Modelling, in press, doi:10.1016/j.apm.2007.11.009.
[9] M. Van Dyke, Perturbation Methods in Fluid Mechanics, The Parabolic Press, Stanford, CA, 1975.